chemistry proceedings

MDPI

Proceeding Paper

Interaction of Biomolecules with Silver Nanoparticles Prepared via Intramolecular Redox Reaction of Ag(I) Complexes as Their Precursors †

Iveta S. Turomsha [1,2], Natalia V. Loginova [1,2,*], Maxim Y. Gvozdev [1], Tatiana V. Koval'chuk-Rabchinskaya [1] and Nikolai P. Osipovich [2]

[1] Faculty of Chemistry, Belarusian State University, 4 Independence Avenue, 220030 Minsk, Belarus; ivetaturomsha@gmail.com (I.S.T.); gvozdevmaximka@gmail.com (M.Y.G.); ktv-chem@mail.ru (T.V.K.-R.)
[2] Research Institute for Physico-Chemical Problems, Belarusian State University, Leningradskaya Str. 14, 220030 Minsk, Belarus; osipovich@bsu.by
* Correspondence: loginonv@gmail.com
† Presented at the 28th International Electronic Conference on Synthetic Organic Chemistry (ECSOC-28), 15–30 November 2024; Available online: https://sciforum.net/event/ecsoc-28.

Abstract: Nanoparticles are known to have a high specific surface area, which accounts for an increased probability of their interaction with bacterial cells. Therefore, the application of silver(I) nanoparticles (AgNPs) and their nanocomposites as antimicrobial agents against drug-resistant bacterial strains appears to be prospective. A critical point for the advancement of AgNPs into clinical practice is a fundamental understanding of their behavior in biological systems, including protein binding and interaction with blood components, which reflects their toxicity. The latter is primarily determined by the physicochemical properties of AgNPs, namely their size, shape, surface chemistry, etc. Therefore, nanotoxicity may be substantially reduced through the manipulation of certain physicochemical characteristics of AgNPs, increasing their biocompatibility and hence paving the way for possible biomedical applications. In this study we have focused on estimating the binding affinity of the synthesized Ag(I) complexes of 2-(4,6-di-*tert*-butyl-2,3-dihydroxyphenylsulfanyl)-acetic acid and 4,6-di-*tert*-butyl-2,3-dihydroxybenzaldehyde isonicotinoyl hydrazone, as well as AgNPs derived thereof to bovine serum albumin (BSA) and hemoglobin by the fluorimetric method. Furthermore, cellular toxicity of the AgNPs towards human erythrocytes was measured in a hemolysis assay. Organosols formed by the Ag(I) complexes upon their reduction to AgNPs in acetonitrile and DMSO were characterized by the transmission electron microscopy (TEM) method and atomic force microscopy (AFM).

Keywords: nanotoxicity; bovine serum albumin; hemoglobin; hemolytic activity

check for updates

Citation: Turomsha, I.S.; Loginova, N.V.; Gvozdev, M.Y.; Koval'chuk-Rabchinskaya, T.V.; Osipovich, N.P. Interaction of Biomolecules with Silver Nanoparticles Prepared via Intramolecular Redox Reaction of Ag(I) Complexes as Their Precursors. *Chem. Proc.* **2024**, *16*, 40. https://doi.org/10.3390/ecsoc-28-20173

Academic Editor: Julio A. Seijas

Published: 14 November 2024

Copyright: © 2024 by the authors. Licensee MDPI, Basel, Switzerland. This article is an open access article distributed under the terms and conditions of the Creative Commons Attribution (CC BY) license (https://creativecommons.org/licenses/by/4.0/).

1. Introduction

Since the synthesis of homogenous nanoparticles of a given size, shape and physicochemical properties is of interest in terms of the development of new therapeutic and diagnostic agents, modern nanotechnologies undoubtedly possess significant potential for medical applications [1–4]. Nanoparticles are characterized by specific physicochemical, biological and pharmacokinetic properties that may be used for the targeted delivery of drugs, prolongation of their therapeutic effect or reducing adverse drug reactions. Nevertheless, there is a lack of information about the nanoparticle-mediated processes that occur in living organisms. Artificial nanoparticles may interact with proteins and nucleic acids, anchor in biological membranes and penetrate into the organelles of the cell, and hence modify the functions of cellular components [5]. Nanoparticles of a size less than 70 nm are not recognized by the defense systems of the human body (namely by macrophages), do not undergo biotransformations and are not eliminated from the organism [6]. Therefore,

the investigation of possible consequences of the interactions that arise upon direct contact of human cells with artificial nanoparticles appears of great importance, considering the fact that the size of the latter is comparable to that of biological nanoobjects in living organisms. Additionally, the risks posed by nanoparticles are further aggravated by the unpredictability of these consequences.

The comprehensive risk assessment system of artificial nanomaterials comprises a wide range of physicochemical, biochemical and toxicological tests as well as special studies that provide an estimate of their impact on biological objects [7,8]. However, the development of a general empirical approach to the evaluation of the safety of artificial nanoparticles in terms of their interaction with biomolecules is required, including investigation of their physicochemical properties, their biological action in vitro and factors relating to their potential nanotoxicity. The latter are primarily determined by the physicochemical properties of the particle surface and by their modification resulting from contact with the environment, biological objects, etc. [7]. These processes are influenced by the chemical and phase composition, structure, shape, size distribution and hydrophilicity (hydrophobicity) of the particles, the presence of certain functional groups on their surface, the properties of the environment, as well as by the solid–liquid and nanoparticle–bioobject interfaces [5,8].

Nanoparticles are known to have a high specific surface area, which accounts for an increased probability of their interaction with bacterial cells [9]. Therefore, the application of AgNPs and their nanocomposites of the size 1–100 nm as antimicrobial agents against drug-resistant bacterial strains appears to be prospective [2,10]. Systematic nanotoxicity studies generally imply the development of proper synthetic rules for the synthesis of safe AgNPs. For this end, a thorough physicochemical characterization of nanoparticles and the investigation of their effects on model systems are necessary. There are various physical, chemical and biological methods for the synthesis of AgNPs summarized in the literature, with their advantages and disadvantages analyzed and the unique biocidal properties of nanoparticles discussed. The latter significantly depend on the size and shape of the nanoparticles and hence on the selected synthetic method [1,2,7].

They include (i) reduction of Ag(I) salts [11], (ii) chemical vapor deposition [12], (iii) decomposition of metal–organic compounds [13,14], (iv) laser ablation [15], (v) microwave synthesis [16] and (vi) electrochemical synthesis [17]. Among them, the synthesis of AgNPs by the decomposition of metal complexes in solution is of special interest, considering the fact that Ag(I) complexes contain all the components necessary for the formation of a stable silver sol: Ag(I) ions act as oxidants, and phenolic compounds act as reductants, whereas the oxidation products of the organic ligands serve as stabilizing agents [18–20].

We have previously conducted the synthesis and physicochemical characterization of two such compounds, namely the Ag(I) complexes of 2-(4,6-di-*tert*-butyl-2,3-dihydroxyphenylsulfanyl)acetic acid (**1**) and 4,6-di-*tert*-butyl-2,3-dihydroxybenzaldehyde isonicotinoyl hydrazone (**2**) [18,19]. Such transition metal complexes of redox-active ligands are characterized by either valent tautomerism or partial charge transfer, implying the intramolecular electron transfer between the ligand and the Ag(I) ion, which leads to the coexistence of both phenol and semiquinone ligand forms [20]. Furthermore, we have proposed the method for the synthesis of AgNPs from the aforementioned Ag(I) complexes by an intramolecular redox reaction in media with high solvation ability ($DN > 19$), such as DMF, DMSO, ethanol, 2-propanol and 2-methylpropan-1-ol [18]. The size of primary AgNPs in the organosol determined by the methods of absorption spectroscopy, transmission electron and atomic force microscopies has been found to be 5–20 nm [18,20]. Moreover, it has been established that the synthesized AgNPs efficiently suppress the growth of bacteria, yeasts and molds at very low concentrations (MIC 0.007 μmol/mL) [20]. Therefore, the results obtained may be of interest in terms of the discovery of novel anti-infective agents possessing both high antibacterial and antifungal activity. An essential property of the synthesized AgNPs is the presence of surface coatings, which may either mitigate or eliminate the adverse effects exerted by nanoparticles [5,7]. Surface coatings have been shown to contribute to

nanoparticle stabilization and prevent their agglomeration, while also being an effective inhibitor of their dissolution and the release of toxic metal ions [7,21]. Additionally, the steric hindrance induced by surface coatings may reduce the uptake and accumulation of nanoparticles by the cell [22]. Nanoparticle surface charge or surface composition modified by the coatings could further influence intracellular distribution and increase the toxicity of nanoparticles due to ROS production [5,7].

In this work we have employed methods measuring the impact of the synthesized AgNPs on various intracellular processes, particularly their interaction with biomolecules (albumin and hemoglobin), for the estimation of their potential in vitro toxicity as well as cell viability. More specifically, hemolysis caused by AgNPs may indicate both their extreme cellular toxicity and membrane disruption, which is crucial for nanoparticles intended to penetrate into the bloodstream as chemotherapeutic agents. Being an extremely sensitive technique, spectrophotometric detection of hemoglobin is used in a wide range of studies investigating the hemolytic potential of functionalized metal nanoparticles [23].

2. Materials and Methods

Solvents (HPLC grade), ligands and their Ag(I) complexes were used without further purification. Synthetic procedures for the ligands, Ag(I) complexes with 2-[4,6-di-(*tert*-butyl)-2,3-dihydroxyphenylsulfanyl]acetic acid (**Complex 1**) and 4,6-di-*tert*-butyl-2,3-dihydroxybenzaldehyde isonicotinoyl hydrazone (**Complex 2**) and their physicochemical characteristics are described in [18,19].

2.1. Physicochemical Characterization

Silver organosols were produced by chemical decomposition of the Ag(I) complex dissolved in an organic solvent (acetonitrile (Honeywell, Charlotte, NC, USA) or DMSO (CHROMASOLV™, Honeywell, Charlotte, NC, USA)) under permanent stirring (**AgNPs-1** from **Complex 1**, **AgNPs-2** from **Complex 2**) [18]. The sols were produced in situ via the intramolecular redox reaction of a complex dissolved in an organic solvent so as to provide a silver concentration in the sol equal to 0.1 mM. The sols were stored in closed, light-tight vessels. Upon requirement, argon was bubbled through the solutions to ensure the absence of oxygen. Silver content in the solid phase was determined using an atomic emission spectrometer with an inductively coupled plasma excitation source (Spectroflame Modula). The instrument EM-125 K was used to determine the size and shape of AgNPs as well as the formation of surface coatings by the TEM method.

2.2. Protein Binding Studies

In the fluorescence quenching experiment, quenching of the tryptophan and tyrosine residues of bovine serum albumin (BSA) (Sigma-Aldrich, Burlington, MA, USA) and bovine hemoglobin (Sigma-Aldrich, Burlington, MA, USA) was carried out by keeping a constant concentration of protein (2 μM) in 5 mM Tris-HCl buffer (Hopax Fine Chemicals, Kaohsiung City, Taiwan) (pH 7.4) with 50 mM NaCl (Sigma-Aldrich, Burlington, MA, USA) in the case of BSA and HBS (Sigma-Aldrich, Burlington, MA, USA) (pH 7.4) for bovine hemoglobin, while varying the concentration of the complexes (0–100 μM). The fluorescence spectra of BSA solution alone and in the presence of Ag(I) complexes were recorded in the range of 310–450 nm upon excitation at 295 nm and emission of tryptophan residues of BSA at 324 nm. The same experiments were conducted for hemoglobin solution upon excitation at 280 nm and emission of tryptophan and tyrosine residues of hemoglobin at 311 nm after each addition of the quencher. Solutions of complexes were prepared in acetonitrile (Honeywell, Charlotte, NC, USA). All experiments were carried out at room temperature. The dissociation constant for a simple 1:1 binding process was determined via non-linear regression analysis [24].

$$\frac{F_0 - F}{F_0 - F_s} = \frac{[P] + [Q] + K_d - \sqrt{([P] + [Q] + K_d)^2 - 4[P][Q]}}{2[P]} \quad (1)$$

F, F_0 and F_s are fluorescence intensities with, without the quencher (complex), and fully bound protein, respectively. K_d is the dissociation constant; [P] and [Q] are concentrations of protein and quencher, respectively. The apparent binding constants (logK_h) and the Hill coefficients (n) were calculated from the plot of log[$(F_0 - F)/F$] versus log[Q] according to the following equation:

$$\log \frac{F_0 - F}{F - F_s} = \log K_h + n \log[Q] \quad (2)$$

2.3. Hemolysis Assay

Human erythrocytes from healthy individuals were collected in tubes containing anticoagulant. The erythrocytes were separated from plasma by centrifugation for 10 min at 2000× g at room temperature. The supernatant was discarded and the pellet was washed once with 0.9% NaCl (Sigma-Aldrich, Burlington, MA, USA) solution and twice with HEPES buffered saline (Sigma-Aldrich, Burlington, MA, USA) (pH 7.4). The 10% suspension of human red blood cells was diluted with HBS (1:10), transferred to the tubes and treated with the compounds under study dissolved in DMSO (CHROMASOLV™, Honeywell, Charlotte, NC, USA) in different concentrations (15–500 μM) at 37 °C for 30 min. The tubes were centrifuged for 10 min at 2000× g at room temperature and the absorbance of supernatant was measured at 550 nm. Control experiments with 1% dimethyl sulfoxide were included. Total hemolysis was achieved with 1% Triton X-100 (Sigma-Aldrich, Burlington, MA, USA). The hemolysis percentage (H) was calculated as follows:

$$H\,(\%) = \frac{A_1 - A_0}{A_{100} - A_0} \times 100\% \quad (3)$$

$A_1$is the absorbance of a sample, A_0 is the absorbance of negative control, and A_{100} is the absorbance of positive control. HC_{10} defines the concentration of the tested compound which induces 10% hemolysis.

3. Results and Discussion

The stability of organosols was shown to be significantly dependent on the nature of the dispersion medium. Morphological characterization of AgNPs was carried out by means of TEM (Figure 1) and AFM (Figure A1). According to the AFM data, the size of the primary AgNPs in organosols falls within the range of 5–10 nm, whereas the objects sized 20–40 nm that were observed on the AFM images have been found to represent aggregates of densely packed AgNPs.

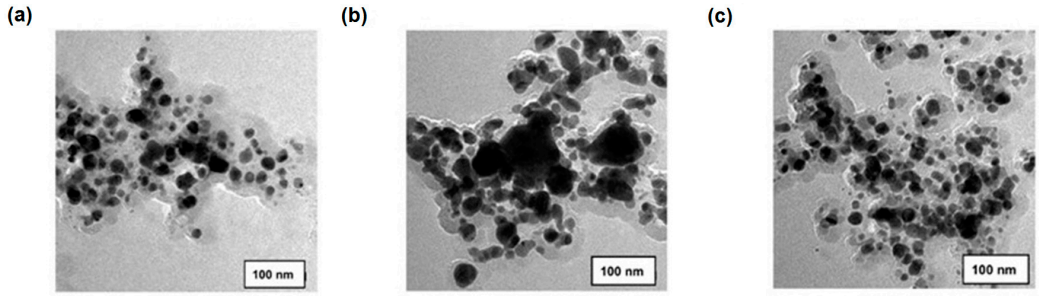


Figure 1. (**a**) TEM images of AgNPs-2 in acetonitrile within 30 min. (**b**) TEM images of AgNPs-2 in acetonitrile within 5 h. (**c**) TEM images of AgNPs-2 in DMSO within 30 min. A more rapid formation of AgNPs-2 is observed in DMSO possessing a higher donor number.

Geometric parameters of the complexes were determined using DFT calculations [19]. The Mulliken orbital population analysis suggests that a substantial change of atomic charge occurs for the coordinated oxygen atoms upon complexation, with these centers being the major participants of partial charge transfer. The plausible general coordination modes for **Complex 1** and **Complex 2** inferred from the DFT calculations are [AgLHL]

and [AgL_2NO_3], respectively, where L is the corresponding ligand (L = 2-(4,6-di-*tert*-butyl-2,3-dihydroxyphenylsulfanyl)-acetic acid for the **Complex 1** and L = 4,6-di-*tert*-butyl-2,3-dihydroxybenzaldehyde isonicotinoyl hydrazone for the **Complex 2**). Structural formulas of the ligands are shown in Figure A2.

Silver organosols were produced by chemical decomposition of the Ag(I) complex dissolved in an organic solvent (acetonitrile or DMSO) under permanent stirring (**AgNPs-1** from Complex 1, **AgNPs-2** from Complex 2). As was mentioned above, physicochemical properties of nanoparticles significantly depend on their physiological environment, which is a consequence of adsorption of biomolecules resulting in the formation of a surface coating called a "protein corona". Such prominent interactions of nanoparticles with serum or plasma proteins occur due to their high surface free energy and surface area to volume ratio and have been reported to influence the processes of nanoparticle toxicity, cellular targeting and clearance in vivo.

Protein binding to the nanoparticle surface correlates with both their mobility (association rates) and abundance in human plasma. The proteins that exhibit higher affinity to the nanoparticle surface are known to constitute the "hard corona", whereas less tightly bound proteins with lower affinity form the "soft corona" [25–29]. The latter interact indirectly with the nanoparticle surface and are readily exchanged during the traveling of nanoparticles through various protein-rich environments in the organism. In this way, initially bound proteins are dynamically replaced by the more abundant proteins with higher affinity, according to the Vroman theory [30]. In contrast to this, since the irreversibly bound "hard corona" remains relatively unaltered in the course of time, the proteins adsorbed upon initial exposure to the biological system continuously mediate the interaction of the nanoparticle with the surrounding cells [31]. Moreover, the protein–nanoparticle interaction is facilitated by the presence of charged functional groups and by the hydrophobicity of the nanoparticle surface. It should also be noted that the biological reactivity of nanoparticles significantly depends on the pattern of protein arrangement on their surface: human serum albumin (HSA) and transferrin tend to form monolayers on nanoparticles, whereas bovine serum albumin (BSA) is capable of forming dimers on their surface [32,33].

Naturally, major constituents of the "protein corona" that are rapidly adsorbed to nanoparticles participate in the physiological processes of pathogen recognition and lipid and ion transport, and complement activation and blood coagulation. Therefore, the most frequent components identified in the "protein corona" include albumin, α-2-macroglobulin, apolipoproteins (apolipoprotein A-I, apolipoprotein A-III and apolipoprotein C-III), immunoglobulins (immunoglobulin kappa chain and forms of light and heavy chains of immunoglobulins), complement factors (complement C3 and complement C4), coagulation factors (kininogen and plasminogen), keratin, vitronectin, haptoglobin, alpha-1-antitrypsin, etc. [25,34,35]. For instance, the adsorption of albumin or apolipoproteins enables the transportation of nanoparticles, whereas the interaction of nanoparticles with complement proteins and immunoglobulins causes particle opsonization and hence facilitates their elimination [36].

Protein binding to the nanoparticle surface involves bond formation, conformational changes of the protein and water molecule rearrangement at the interface that imply changes both in enthalpy and entropy of the system. Adsorption of protein macromolecules onto the nanoparticle may imply hydrogen bond formation in specific domains, as well as non-specific Van der Waals interactions and solvation forces [29]. Changes in the protein conformation frequently result from the interaction of either charged amino acid sequences or hydrophobic patches within the protein structure with the nanoparticle surface, rendering such a process thermodynamically favorable [37]. For several proteins, particularly HSA, a decrease in enthalpy is observed in an exothermic binding process with nanoparticles. However, for fibrinogen, ovalbumin, human carbonic anhydrase II and lysozyme, no enthalpy changes occur upon their interaction with nanoparticles, suggesting that the binding process is an entropy-driven mechanism that depends on the rearrangement of the bound interfacial water molecules and does not induce any

conformational changes of the protein [38]. Furthermore, conformational changes in the protein structure could result solely from the nanoparticle itself: gold nanoparticles have been shown to induce conformational changes in BSA in a dose-dependent manner, whereas in the case of carbon C_{60} fullerene nanoparticles the conformation of BSA remained intact [39,40].

3.1. Albumin Binding Studies

Since the commercially available BSA protein is known to possess 76% structural homology to the HSA protein, experimentally determined binding parameters of metal complexes to BSA could be extrapolated to the case of HSA [41]. Interaction of the complexes with BSA was investigated by monitoring the native fluorescence intensity of the tryptophan residues Trp134 and Trp212 at the wavelength of 328 nm [42]. Fluorescence quenching of BSA observed for the metal complexes both in acetonitrile and DMSO may refer either to the changes in the protein conformation in the 124–298 region as a result of protein complex interaction or to π–π stacking interactions of the ligands with aromatic fragments of tryptophan [43,44]. It has been demonstrated that the dissociation constants of the protein–metal complex conjugate decrease upon the formation of nanoparticles in DMSO, whereas the Hill coefficients and binding constant logarithms remain unchanged (Table 1). The increase in binding affinity for BSA observed for nanoparticles compared to their molecular forms present in acetonitrile solution could be referred to the formation of a "protein corona" on the nanoparticle surface as an additional mechanism of protein binding. Considering the fact that the nanoparticles formed in DMSO are primarily coated by the oxidized form of the ligand resulting from an intramolecular reduction of Ag(I), the corona could be acquired by nanoparticles via hydrogen bond formation involving quinone carbonyl groups, as well as by Van der Waals forces.

Table 1. Albumin binding of the silver(I) complexes in acetonitrile and DMSO media.

Compound	K_d, M^{-1}	n	logK_h
Complex 1	$(6.87 \pm 0.90) \times 10^{-6}$	1.20 ± 0.10	6.02 ± 0.51
AgNPs-1	$(3.19 \pm 0.53) \times 10^{-6}$	1.15 ± 0.07	6.16 ± 0.38
Complex 2	$(5.09 \pm 1.01) \times 10^{-6}$	0.97 ± 0.13	5.10 ± 0.69
AgNPs-2	$(1.15 \pm 0.29) \times 10^{-6}$	0.90 ± 0.16	5.18 ± 0.81

3.2. Hemoglobin Binding Studies

Serving as an oxygen transport protein located in erythrocytes, hemoglobin is a crucial component of the human blood transport system. Hemoglobin is known to possess a quaternary structure that comprises two α,β-dimers. The native fluorescence of hemoglobin is considered to result from the tryptophan residue at the β-37 position located at the interface between two dimers [45]. In contrast to BSA, hemoglobin has been shown to bind more readily to the molecular forms of silver(I) complexes in acetonitrile in comparison with the corresponding nanoparticles formed in DMSO (Table 2). This could be due to the bulky quaternary structure of hemoglobin that is not capable of interacting efficiently with the surface of silver nanoparticles coated by the oxidized molecules of sterically hindered ligands, which renders the entropy-driven binding process less thermodynamically favorable. Therefore, an increase in dissociation constants is observed upon transition from acetonitrile to DMSO in the case of hemoglobin.

Table 2. Hemoglobin binding of the silver(I) complexes in acetonitrile and DMSO media.

Compound	K_d, M^{-1}	n	$\log K_h$
Complex 1	$(2.94 \pm 0.38) \times 10^{-5}$	0.99 ± 0.06	4.48 ± 0.29
AgNPs-1	$(4.93 \pm 0.92) \times 10^{-5}$	0.83 ± 0.07	3.53 ± 0.38
Complex 2	$(2.29 \pm 0.34) \times 10^{-6}$	0.84 ± 0.06	3.46 ± 0.31
AgNPs-2	$(6.97 \pm 0.67) \times 10^{-6}$	1.10 ± 0.05	5.67 ± 0.25

3.3. Hemolytic Activity

Since the necrosis of erythrocytes caused by potential chemotherapeutic agents indicates the cell toxicity of the latter, investigation of hemolytic activity of nanoparticles appears relevant. Plausible mechanisms of the induction of hemolysis mainly imply the interaction of erythrocyte membrane lipids with the tested compounds. Since there is frequently a direct correlation observed between hemolytic activity and the lipophilicity of compounds, the formation of metal complexes is likely to cause an increase in hemolytic activity due to an enhancement in the hydrophobicity of organic ligands [46]. In this interconnection, the determination of hemolytic activity of silver(I) complexes appears necessary to estimate their applicability in medicine. HC_{10} values of the tested compounds have been found to exceed 500 μM, which indicates their low hemolytic activity.

4. Conclusions

The present study suggests that the interaction of the synthesized silver(I) complexes with BSA and hemoglobin is mainly affected by either their molecular or nanoparticle nature, as well as by the presence of surface coatings on the formed AgNPs and the conformational characteristics of the protein corona. Understanding the crucial determinants of protein binding by AgNPs may shed light on both their bioavailability and biocompatibility, thereby providing necessary information on their efficacy and safety in biomedical and therapeutic applications. Our study illustrates that seemingly insignificant changes in the surface chemistry of the nanoparticles, namely their surface functionalization via the formation of a surface coating by the oxidized form of the ligand, may exert reasonable effects on their toxicity. It has been shown that surface coatings substantially decrease the toxicity of AgNPs towards erythrocytes, which results in their low hemolytic activity.

However, there still remains a need to gain a more comprehensive insight into the influence of the surface chemistry of AgNPs on their overall toxicity in order to reliably predict their behavior upon possible biological exposure.

Author Contributions: Conceptualization, N.V.L.; methodology, M.Y.G. and N.V.L.; software, T.V.K.-R.; validation, M.Y.G.; formal analysis, I.S.T. and N.V.L.; investigation, I.S.T.; resources, N.P.O.; data curation, I.S.T.; writing—original draft preparation, I.S.T.; writing—review and editing, N.V.L.; visualization, I.S.T. and T.V.K.-R.; supervision, T.V.K.-R. and N.V.L.; project administration, N.V.L.; funding acquisition, N.V.L. All authors have read and agreed to the published version of the manuscript.

Funding: This research received no external funding.

Institutional Review Board Statement: Not applicable.

Informed Consent Statement: Not applicable.

Data Availability Statement: The dataset is available on request from the authors.

Acknowledgments: The work was carried out within the framework of task 2.2.01.05 SRP "Chemical processes, reagents and technologies, bioregulators and bioorganic chemistry".

Conflicts of Interest: The authors declare no conflicts of interest.

Appendix A

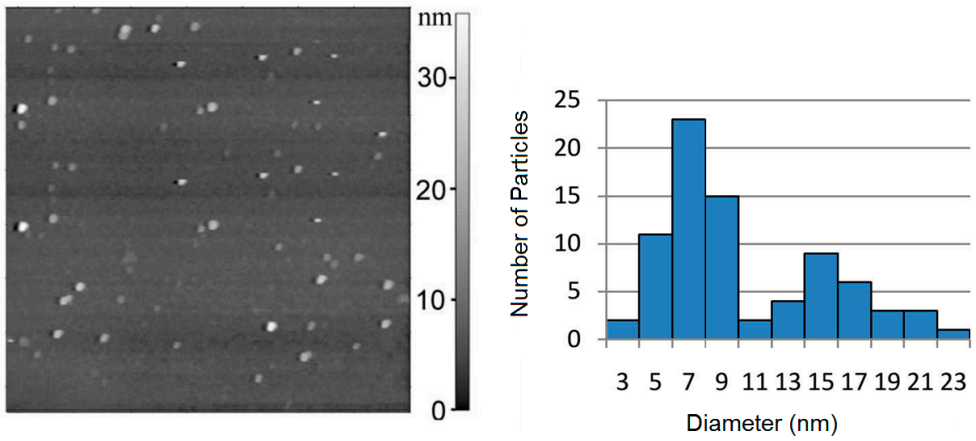


Figure A1. AFM image, and size distribution of the AgNPs.

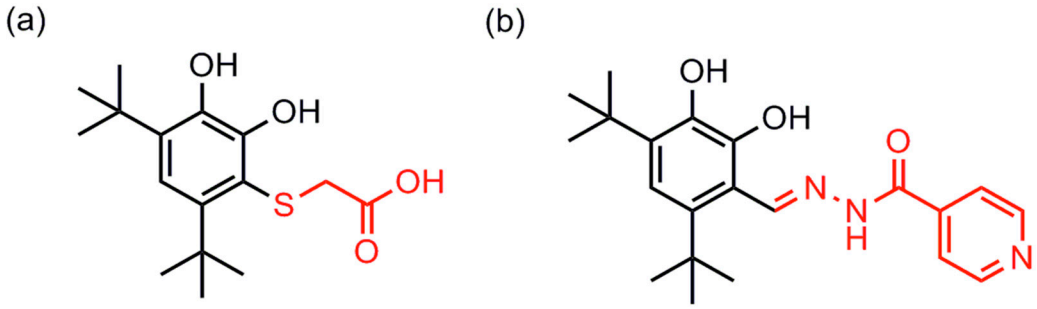


Figure A2. Structural formulas of the ligands of the Ag(I) complexes: (**a**) 2-(4,6-di-*tert*-butyl-2,3-dihydroxyphenylsulfanyl)-acetic acid; (**b**) 4,6-di-*tert*-butyl-2,3-dihydroxybenzaldehyde isonicotinoyl hydrazone.

References

1. Neelgund, G.M.; Karthikeyan, B.; Shivashankar, S.A.; Oki, A. Single-step, size-controlled synthesis of colloidal silver nanoparticles stabilized by octadecylamine. *Appl. Surf. Sci.* **2015**, *356*, 726–731. [CrossRef]
2. Cao, H. *Silver Nanoparticles for Antibacterial Devices Biocompatibility and Toxicity*, 1st ed.; CRC Press: Boca Raton, FL, USA, 2017.
3. Stoeva, S.I.; Huo, F.; Lee, J.S.; Mirkin, C.A. Three-Layer Composite Magnetic Nanoparticle Probes for DNA. *J. Am. Chem. Soc.* **2005**, *127*, 15362–15363. [CrossRef] [PubMed]
4. Cheng, C.-S.; Chen, Y.-Q.; Lu, C.-J. Organic vapour sensing using localized surface plasmon resonance spectrum of metallic nanoparticles self assemble monolayer. *Talanta* **2007**, *73*, 358–365. [CrossRef] [PubMed]
5. Nel, A.E.; Madler, L.; Velegol, D.; Xia, T.; Hoek, E.M.V.; Somasundaran, P.; Klaessig, F.; Castranova, V.; Thompson, M. Understanding Biophysicochemical Interactions at the Nano-Bio Interface. *Nat. Mater.* **2009**, *8*, 543–557. [CrossRef]
6. Moein Moghimi, S.; Shadi Farhangrazi, Z. Nanoparticles in Medicine: Nanoparticle Engineering for Macrophage Targeting and Nanoparticles that Avoid Macrophage Recognition. In *Nanoparticles and the Immune System. Safety and Effects*, 1st ed.; Boraschi, D., Duschl, A., Eds.; Academic Press: New York, NY, USA, 2014; pp. 77–89. [CrossRef]
7. Sharifi, S.; Behzadi, S.; Laurent, S.; Forrest, M.L.; Stroeve, P.; Mahmoudi, M. Toxicity of nanomaterials. *Chem. Soc. Rev.* **2012**, *41*, 2323–2343. [CrossRef]
8. Love, S.A.; Maurer-Jones, M.A.; Thompson, J.W.; Lin, Y.-S.; Haynes, C.L. Assessing Nanoparticle Toxicity. *Annu. Rev. Anal. Chem.* **2012**, *5*, 181–205. [CrossRef]
9. Rai, M.; Yadav, A.; Gade, A. Silver Nanoparticles as a New Generation of Antimicrobials. *Biotechnol. Adv.* **2009**, *27*, 76–83. [CrossRef]
10. Lansdown, A.B.G. *Silver in Health Care: Antimicrobial Effects and Safety in Use*; RCS: Cambridge, UK, 2010.
11. Guzman, M.; Dille, J.; Godet, S. Synthesis and antibacterial activity of silver nanoparticles against gram-positive and gram-negative bacteria. *Nanomed. Nanotechnol. Biol. Med.* **2012**, *8*, 37–45. [CrossRef]
12. Zhang, X.; Xu, S.; Jiang, S.; Wang, J.; Wei, J.; Xu, S. Growth graphene on silver–copper nanoparticles by chemical vapor deposition for high-performance surface-enhanced Raman scattering. *Appl. Surf. Sci.* **2015**, *353*, 63–70. [CrossRef]
13. Hosseinpour-Mashkani, S.M.; Ramezani, M. Silver and silver oxide nanoparticles: Synthesis and characterization by thermal decomposition. *Mater. Lett.* **2014**, *130*, 259–262. [CrossRef]

14. Soayed, A.A. Preparation, characterization and biological activity of silver nanoparticles and silver (I) complex using the new compound 2, 2′-(2-phenyl acetylazanediyl) diacetic acid. *Inorganica Chim. Acta* **2015**, *429*, 257–265. [CrossRef]
15. Valverde-Alva, M.A.; García-Fernández, T.; Villagrán-Muniz, M.; Sánchez-Aké, C.; Castañeda-Guzmán, R.; Esparza-Alegría, E. Synthesis of silver nanoparticles by laser ablation in ethanol: A pulsed photoacoustic study. *Appl. Surf. Sci.* **2015**, *355*, 341–349. [CrossRef]
16. El-Naggar, M.E.; Shaheen, T.I.; Fouda, M.M.G.; Hebeish, A.A. Eco-friendly microwave-assisted green and rapid synthesis of well-stabilized gold and core-shell silver-gold nanoparticles. *Carbohydr. Polym.* **2016**, *136*, 1128–1136. [CrossRef]
17. Nasretdinova, G.R.; Osin, Y.N.; Gubaidullin, A.T.; Yanilkin, V.V. Methylviologen Mediated Electrosynthesis of Palladium Nanoparticles Stabilized with CTAC. *J. Electrochem. Soc.* **2015**, *50*, 69–72. [CrossRef]
18. Loginova, N.V.; Chernyavskaya, A.A.; Parfenova, M.S.; Osipovich, N.P.; Polozov, G.I.; Fedutik, Y.A. Complex of silver (I) with 2-[4,6-di(tert-butyl)-2,3-dihydroxyphenylsulfanyl]acetic acid as a precursor of silver nanoparticles. *Polyhedron* **2006**, *25*, 1723–1728. [CrossRef]
19. Loginova, N.V.; Koval'chuk, T.V.; Gres, A.T.; Osipovich, N.P.; Polozov, G.I.; Halauko, Y.S. Redox-active metal complexes of sterically hindered phenolic ligands: Antibacterial activity and reduction of cytochrome c. Part IV. Silver(I) complexes with hydrazone and thiosemicarbazone derivatives of 4,6-di-tert-butyl-2,3-dihydroxybenzaldehyde. *Polyhedron* **2015**, *88*, 125–137. [CrossRef]
20. Loginova, N.; Gvozdev, M.; Osipovich, N.; Khodosovskaya, A.; Kovalchuk-Rabchinskaya, T.; Ksendzova, G.; Kotsikau, D.; Evtushenkov, A. Silver(I) complexes with phenolic Schiff bases: Synthesis, antibacterial evaluation and interaction with biomolecules. *ADMET DMPK* **2022**, *10*, 197–212. [CrossRef]
21. Kirchner, C.; Liedl, T.; Kudera, S.; Pellegrino, T.; Javier, A.M.; Gaub, H.E.; Stozle, S.; Fertig, N.; Parak, W.J. Cytotoxicity of colloidal CdSe and CdSe/ZnS nanoparticles. *Nano Lett.* **2005**, *5*, 331–338. [CrossRef]
22. Otsuka, H.; Nagasaki, Y.; Kataoka, K. PEGylated nanoparticles for biological and pharmaceutical applications. *Adv. Drug Deliv. Rev.* **2003**, *55*, 403–419. [CrossRef]
23. Lin, Y.-S.; Haynes, C.L. Synthesis and characterization of biocompatible and size-tunable multifunctional porous silica nanoparticles. *Chem. Mater.* **2009**, *21*, 3979–3986. [CrossRef]
24. Beckett, D. Measurement and Analysis of Equilibrium Binding Titrations: A Beginner's Guide. *Methods Enzymol. Meth Enzymol.* **2011**, *488*, 1–16. [CrossRef]
25. Cedervall, T.; Lynch, I.; Foy, M.; Berggad, T.; Donnelly, S.; Cagney, G.; Linse, S.; Dawson, K. Detailed identification of plasma proteins adsorbed on copolymer nanoparticles. *Angew. Chem. Int. Ed.* **2007**, *46*, 5754–5756. [CrossRef] [PubMed]
26. Landsiedel, R.; Ma-Hock, L.; Kroll, A.; Hahn, D.; Schnekenburger, J.; Wiench, K.; Wohlleben, W. Testing Metal-Oxide Nanomaterials for Human Safety. *Adv. Mater.* **2010**, *22*, 2601–2627. [CrossRef]
27. Lundqvist, M.; Sethson, I.; Jonsson, B.-H. Protein Adsorption onto Silica Nanoparticles: Conformational Changes Depend on the Particles' Curvature and the Protein Stability. *Langmuir* **2004**, *20*, 10639–10647. [CrossRef]
28. Lundqvist, M.; Sethson, I.; Jonsson, B.-H. Transient Interaction with Nanoparticles "Freezes" a Protein in an Ensemble of Metastable Near-Native Conformations. *Biochemistry* **2005**, *44*, 10093–10099. [CrossRef]
29. Karajanagi, S.S.; Vertegel, A.A.; Kane, R.S.; Dordick, J.S. Structure and Function of Enzymes Adsorbed onto Single-Walled Carbon Nanotubes. *Langmuir* **2004**, *20*, 11594–11599. [CrossRef]
30. Saptarshi, S.R.; Duschl, A.; Lopata, A.L. Interaction of nanoparticles with proteins: Relation to bio-reactivity of the nanoparticle. *J. Nanobiotechnology* **2013**, *11*, 26. [CrossRef]
31. Maiolo, D.; Bergese, P.; Mahon, E.; Dawson, K.A.; Monopoli, M.P. Surfactant titration of nanoparticle–protein corona. *Anal. Chem.* **2014**, *86*, 12055–12063. [CrossRef]
32. Jiang, X.; Weise, S.; Hafner, M.; Rocker, C.; Zhang, F.; Parak, W.J.; Nienhaus, G.U. Quantitative analysis of the protein corona on FePt nanoparticles formed by transferrin binding. *J. R. Soc. Interface* **2009**, *7*, S5–S13. [CrossRef]
33. Rezwan, K.; Meier, L.P.; Rezwan, M.; Vörös, J.; Textor, M.; Gauckler, L.J. Bovine Serum Albumin Adsorption onto Colloidal Al_2O_3 Particles: A New Model Based on Zeta Potential and UV–vis Measurements. *Langmuir* **2004**, *20*, 10055–10061. [CrossRef]
34. Lundqvist, M.; Stigler, J.; Elia, G.; Lynch, I.; Cedervall, T.; Dawson, K.A. Nanoparticle size and surface properties determine the protein corona with possible implications for biological impacts. *Proc. Natl. Acad. Sci. USA* **2008**, *105*, 14265–14270. [CrossRef] [PubMed]
35. Tenzer, S.; Docter, D.; Rosfa, S.; Wlodarski, A.; Kuharev, J.; Rekik, A.; Knauer, S.K.; Bantz, C.; Nawroth, T.; Bier, C.; et al. Nanoparticle size is a critical physicochemical determinant of the human blood plasma corona: A comprehensive quantitative proteomic analysis. *ACS Nano* **2011**, *5*, 7155–7167. [CrossRef] [PubMed]
36. Owens, D.E.; Peppas, N.A. Opsonization, biodistribution, and pharmacokinetics of polymeric nanoparticles. *Int. J. Pharm.* **2006**, *307*, 93–102. [CrossRef] [PubMed]
37. Chakraborty, S.; Joshi, P.; Shanker, V.; Shanker, V.; Ansari, Z.A.; Singh, S.P.; Chakrabarti, P. Contrasting effect of gold nanoparticles and nanorods with different surface modifications on the structure and activity of bovine serum albumin. *Langmuir* **2011**, *27*, 7722–7731. [CrossRef] [PubMed]
38. Lynch, I.; Dawson, K.A. Protein-nanoparticle interactions. *Nano Today* **2008**, *3*, 40–47. [CrossRef]
39. Treuel, L.; Brandholt, S.; Maffre, P.; Wiegele, S.; Shang, L.; Nienhaus, G.U. Impact of protein modification on the protein corona on nanoparticles and nanoparticle–cell interactions. *ACS Nano* **2014**, *8*, 503–513. [CrossRef]

40. Gessner, A.; Lieske, A.; Paulke, B.R.; Paulke, B.; Müller, R. Influence of surface charge density on protein adsorption on polymeric nanoparticles: Analysis by twodimensional electrophoresis. *Eur. J. Pharm. Biopharm.* **2002**, *54*, 165–170. [CrossRef]
41. He, X.M.; Carter, D.C. Atomic structure and chemistry of human serum albumin. *Nature* **1992**, *358*, 209–215. [CrossRef]
42. Silva, D.; Cortez, C.M.; Louro, S.R.W. Quenching of the intrinsic fluorescence of bovine serum albumin by chlorpromazine and hemin. *Braz. J. Med. Biol.* **2004**, *37*, 963–968. [CrossRef]
43. Hrkal, Z.; Kodíček, M.; VodrÁžka, Z.; Meloun, B.; Morávek, L. Hemin binding to human serum albumin and to the three large cyanogen bromide albumin fragments. *Int. J. Biochem.* **1978**, *9*, 349–355. [CrossRef]
44. Kragh-Hansen, U. Molecular aspects of ligand binding to serum albumin. *Pharmacol. Rev.* **1981**, *33*, 17–53. [PubMed]
45. Sengupta, B.; Chakraborty, S.; Crawford, M.; Taylor, J.M.; Blackmon, L.E.; Biswas, P.K.; Kramer, W.H. Characterization of Diadzein-Hemoglobin Binding using Optical Spectroscopy and Molecular Dynamics Simulations. *Int. J. Biol. Macromol.* **2012**, *51*, 250–258. [CrossRef] [PubMed]
46. Yoshikawa, H. Mechanism of haemolysis caused by various substances. *Ind. Health* **1964**, *2*, 155–161. [CrossRef]

Disclaimer/Publisher's Note: The statements, opinions and data contained in all publications are solely those of the individual author(s) and contributor(s) and not of MDPI and/or the editor(s). MDPI and/or the editor(s) disclaim responsibility for any injury to people or property resulting from any ideas, methods, instructions or products referred to in the content.